JOURNAL OF AIRCRAFT
Vol. 30, No. 6, Nov.–Dec. 1993

Thermoacoustic Loads and Fatigue of Hypersonic Vehicle Skin Panels

Robert D. Blevins* and Ian Holehouse†
Rohr Industries, Chula Vista, California 92012
and
Kenneth R. Wentz‡
Wright Research and Development Center, Wright-Patterson Air Force Base, Ohio 45433

A thermo-vibro-acoustic analysis of skin panels for airbreathing hypersonic vehicles is made for a generic trajectory and vehicle design. Aerothermal analysis shows that impingement of the bow shock wave on the vehicle produces fluctuating pressures, and local heat fluxes greatly exceed those due to the attached turbulent boundary. Thermal analysis of carbon-carbon skin panels shows that maximum temperatures will exceed 2700°F (1480°C) at the top of the ascent trajectory. Engine acoustic analysis indicates that sound levels will exceed 170 dB. As a result, loads due to engine acoustics and shock impingement dominate the design of many transatmospheric vehicle skin panels.

Introduction

THERMAL, acoustic, engine, material, and performance issues are interdependent in the design of airbreathing hypersonic vehicles. It is necessary to consider the mission, the trajectory, and the vehicle before analyzing individual skin panels. This article identifies a generic blended wing body (BWB) vehicle that is representative of the single-state-to-orbit transatmospheric vehicles currently being considered in the U.S.[1,2] Aeroacoustic loads and engine-induced loads on the skin are then determined. Thermal, static, and dynamic skin panel responses are found using finite element methods.

The mission objectives of the hypersonic vehicle are to 1) reach orbit with a single stage vehicle, and 2) maintain hypersonic cruise using primarily airbreathing engines. Airbreathing engines demand oxygen to burn fuel. To obtain sufficient oxygen from the atmosphere for combustion, air entering the engine must be at a total pressure (static plus dynamic) of at least 200 lb/ft^2 (10,000 Pa). On the other hand excessive vehicle speed in the atmosphere causing inlet dynamic air pressure beyond 2600 lb/ft^2 (125,000 Pa) penalizes the vehicle by increasing the weight of engine structure required to contain the high inlet pressure. Usable airbreathing flight trajectories fall between these high and low pressure limits and the orbital velocity of Mach 25 as shown in Fig. 1.

To rise to orbit at 200,000 ft (60,000 m) with Mach 25 orbital velocity using airbreathing propulsion, the vehicle must maintain inlet ram air pressure in the usable combustion range while reaching hypersonic speeds in the Earth's atmosphere. Hypersonic flight in the atmosphere causes aerothermal heating of the vehicle skin. This aerothermal heating is considerably more severe for hypersonic air-breathing vehicles than for orbital rockets which carry oxygen internally and reach hypersonic speed above the Earth's atmosphere.[3]

This study considers ascent, cruise, and descent trajectories which are characteristic of recent studies of airbreathing transatmospheric vehicles. Two ascent trajectories were analyzed; $1000q$ and $2600q$, where q is the dynamic pressure of the incoming air in pounds per square foot that the vehicle maintains during ascent. Both ascent trajectories are plotted in Fig. 1. Time to orbit is 15 min, and the acceleration of the vehicle is assumed to be a constant 0.93 g, where g is the acceleration due to gravity at the Earth's surface. Once the vehicle reaches Mach 25 in the atmosphere, final ascent to orbit beyond the atmosphere can be accomplished using small booster rockets.

For a given vehicle Mach number, the dynamic pressure q is higher in the dense air of lower altitudes. For the same Mach number, the $2600q$ ascent trajectory is at lower altitudes and in denser air than the $1000q$ ascent. During both ascents, aerothermal heat fluxes will cause high skin temperatures. To reduce the heat flux and slow down the rate of skin panel temperature rise, the vehicle must gain altitude into less dense air as speed increases. This is shown by the isothermal skin trajectory lines in Fig. 1.

Descent from orbit is made with the airbreathing engines shut down at $200q$ in a trajectory similar to the descent trajectory of the Space Shuttle (Fig. 1). Time to descend from orbit is 45 min. Since aerothermal heat flux on the skin in-

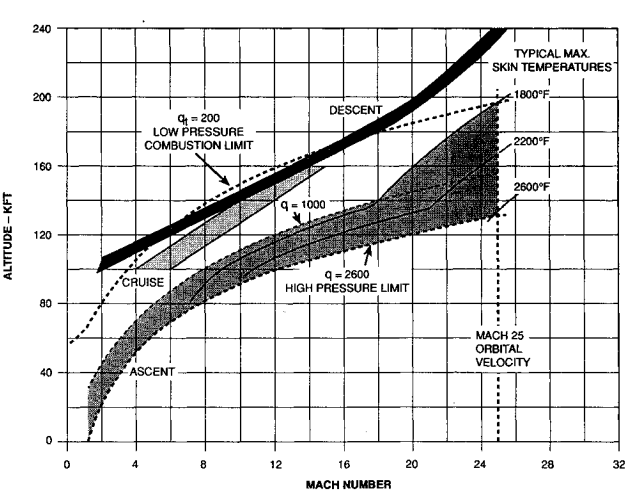

Fig. 1 Transatmospheric vehicle flight trajectories. The air breathing combustion flight envelope is bounded by a total pressure of q_t = 200 lb/ft^2 (10,000 Pa) and a dynamic pressure of q = 2600 lb/ft^2 (150,000 Pa).[2]

Received Dec. 21, 1990; revision received July 9, 1992; accepted for publication July 28, 1992.

*Chief Structural Dynamics, M/S 29T, P.O. Box 878.
†Engineering Staff Specialist, Rohr Industries, M/S 29T, P.O. Box 878.
‡Aerospace Engineer, Acoustic/Sonic Fatigue, Air Force Wright Aeronautical Laboratories, Acoustics and Sonic Fatigue Group, AFWAL/FIBGD. Member AIAA.

creases with vehicle speed and with air density, the 2600q ascent is more severe than the 1000q ascent, and both ascents are more severe than the 200q descent for skin panel loading.[3]

Description of the Vehicle and Skin Panels

Optimized airbreathing transatmospheric vehicle design concepts are driven by the single-stage-to-orbit objective, and the need to carry large volumes of cryogenic liquid hydrogen fuel. Designs currently being considered have large twin horizontal and vertical control surfaces, engines located on the lower midbody, an integrated aftbody nozzle, similar length/width/height ratios, and broad, nearly flat wing and tail control surfaces. Fuel is contained within a conformal, internally braced multibubble tank. The BWB hypersonic transatmospheric vehicle design (Fig. 2) was selected for generic analysis. To increase internal fuel capacity (about 60% of gross takeoff weight is fuel), recent transatmospheric vehicle designs are evolving toward a somewhat heavier vehicle with stockier lines than those of the BWB of Fig. 2. However, the BWB twin tail and lower midbody engine configuration remains the baseline for most studies.

The BWB vehicle has an overall length of approximately 100 ft (30 m), and has a 150,000 lb (68,000 kg) gross weight. The BWB can be divided into the following eight areas: 1) upper forebody [8–30 ft (2.4–9.2 m) aft of nose]; 2) upper midbody [30–60 ft (9.2–18 m) aft of nose]; 3) upper aftbody [60–100 ft (18–30 m) aft of nose]; 4) lower forebody [4–35 ft (1.2–11 m) aft of nose]; 5) engine inlet ramps [35–60 ft (11–18 m) aft of nose]; 6) engine and nozzle [70–100 ft (21–30 m)]; 7) wing, i.e., horizontal surfaces; and 8) vertical stabilizer surfaces. Location of the engine is important. Unlike missiles, the BWB hypersonic vehicle has airbreathing scramjet engines placed at midbody. This allows the vehicle forebody to act as a compression surface for the inlet and the aft body to be an expansion nozzle for the exhaust. The disadvantage of midbody engine placement is that the aftbody vehicle skin is exposed directly to engine acoustic radiation.

The high temperatures of hypersonic vehicle skin panels require unconventional mateials. Conventional high-temperature aluminum alloys such as 2219 Al have upper working temperatures of 350°F (175°C), but may be used to 500°F (260°C) for limited periods of time with some degradation of properties. High-temperature titanium alloys such as Ti-6 Al-2Sn-4Zr-2Mo have a nominal maximum temperature limit of 1000°F (540°C), but recent test suggest that they may be used to 1200°F (650°C) if exposure duration is limited to forestall phase changes and creep. Nickel- and iron-based superalloys are limited by oxidation and creep beyond 1800°F (980°C).

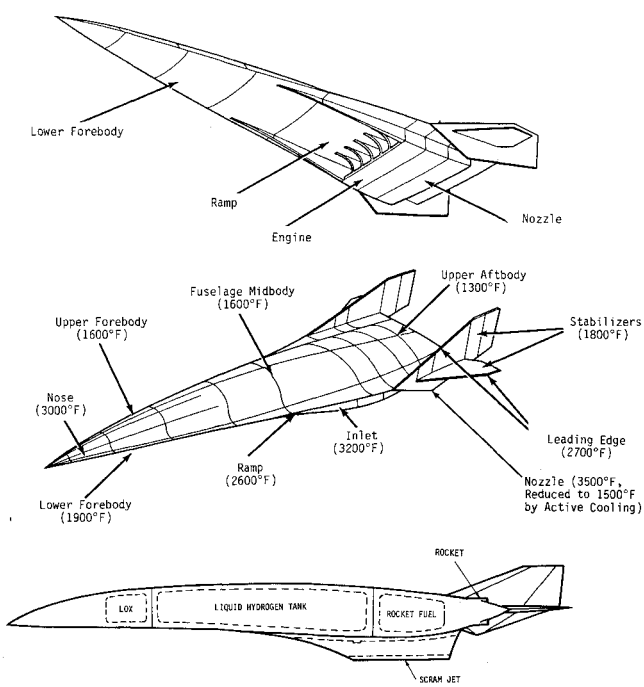

Fig. 2 Blended wing body transatmospheric vehicle design concept.[2]

Silicon and carbon ceramics are capable of temperatures in excess of 2000°F (1090°C). In homogenous solid form, these ceramics are too brittle and damage-sensitive for use as primary structure. Composites with carbon or silicon fibers in a ductile matrix have the toughness and maximum temperatures capability to allow their use for primary vehicle structure. Three ceramic composites were considered for vehicle skin panels: 1) TMC, 2) Si-C, and 3) carbon-carbon. Titanium-metal-matrix composites (TMC) have silicon carbide ceramic fibers in a ductile titanium matrix, Si-C composites have silicon carbide fibers in a carbon matrix, and carbon-carbon has carbon fibers in a carbon matrix. Because they can bear high load while simultaneously withstanding high temperatures, these three ceramic composites allow for a more weight-efficient design of hypersonic vehicle skin panels than the Space Shuttle construction of ceramic heat shields over an aluminum load bearing structure.

Carbon and silicon carbide fiber composites are generally limited by the temperature capability of the matrix rather than the strength of the fiber. Oxidation, the spontaneous combination of atmospheric oxygen with a carbon matrix to form gaseous CO_2, is a common high-temperature failure mode of carbon matrix composites. Silicon carbide glass coatings, applied at high temperature by gaseous diffusion or by direct surface compaction of powder, have been developed to inhibit the penetration of atmospheric oxygen into carbon-carbon. Powdered oxidation inhibitors can be added to the carbon matrix to retard oxidation if the coating becomes damaged. Metallic composites also suffer from oxidation at high temperature if coatings are not applied. Current generation titanium matrix alloys, such as 15V-3Cr Ti, are degraded by oxidation and creep above 1000°F (540°C). Metastable beta titanium alloys such as beta-21S are being developed to improve oxidation properties of TMC.

Skin panels representative of the BWB hypersonic vehicle (Fig. 2) were designed and fabricated as part of a study of aero-thermal-acoustic fatigue of hypersonic vehicles.[2] Carbon-carbon was chosen for the forebody and the ramp skin panels because of thermal and weight considerations. The maximum forebody skin temperatures are greater than the upper-use temperature for advanced titanium matrix composites, but within the temperature range of carbon-carbon. Tradeoff studies have shown that structural carbon-carbon is more weight efficient than actively cooled metallic structures for areas where carbon-carbon use temperature is not exceeded. The lower forebody panel is shown in Fig. 3. The carbon-carbon laminate consists primarily of 0 deg/90 deg plies of carbon-carbon fabric sandwiched between two outer plies of fabric oriented at 45 deg. The 45-deg fabric plies were included to increase buckling allowables.

The skin thickness of the carbon-carbon forebody panel is 0.15 in. (3.8 mm). The stiffener height and thickness of the uniaxial blade stiffeners are 2 in. (5.1 cm) and 0.115 in. (0.29 cm), respectively, and they are spaced at 6-in. (15-cm) intervals. The blade stiffeners taper off into thickened side rails (Fig. 3) to avoid the unacceptable interlaminar stress that would result if the blades were tied directly into the side rails. The blade-type stiffener is chosen because it avoids the reentrant corners of Z-, T-, and hat-stiffeners which cannot be coated with silicon carbide glass to inhibit oxidation. A layer of alumina insulation between the panel and the substructure minimizes heat transfer into the cryogenic hydrogen tank.

The ramp panel is similar in design to the forebody panel. However, since the ramp panel functions primarily as a heat shield and does not bear inplane loads, it has a wider stiffener

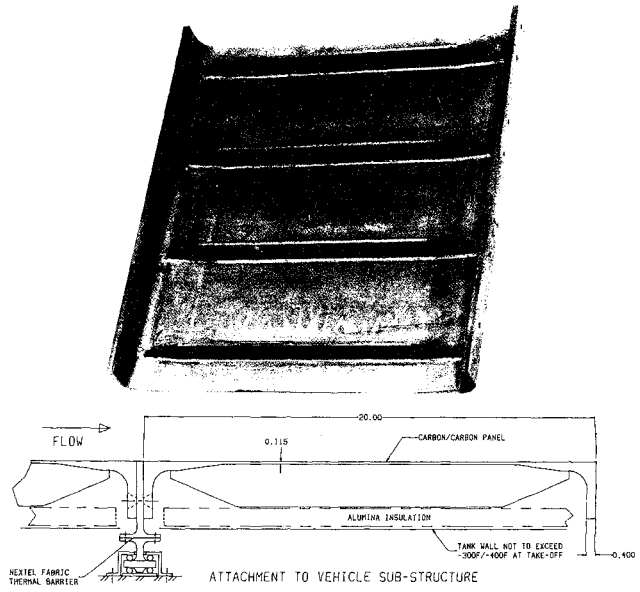

Fig. 3 Carbon-carbon lower forebody panel.

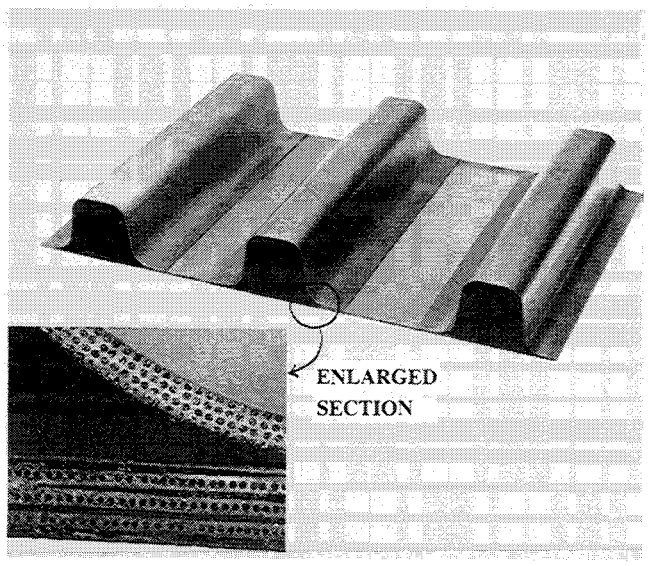

Fig. 4 Titanimum metal matrix prototype wing skin panel. The silcon carbide fibers in the 15V-3Cr titanium matrix are 0.006 in. (0.15 mm) in diameter.

spacing (10 in., 25.4 cm) and a lower skin thickness (0.065 in., 1.65 mm) to minimize weight.

The upper fuselage midbody and aftbody skin are single-faced corrugated panels formed from advanced TMC. Typically the panels are 4 by 4 ft (1.2 by 1.2 m) with 32 corrugated stiffeners per panel. The panels are attached to underlying titanium ring frames and longerons. TMC was chosen for midbody and aftbody skin panels because it has the stiffness required to resist local panel buckling (the failure mode for much of the midbody) while withstanding the midbody skin temperatures.

The wings and vertical stabilizers are also fabricated from advanced titanium metal matrix composite with corrugation-stiffened single skins which are separated by I-section spars. The corrugations are on 1.7-in. (4.3-cm) centers and are 2.5 in. (6.35 cm) in height. All webs and flanges are 0.015 in. (0.38 mm) thick—the minimum gauge for TMC. Figure 4 shows a prototype of a TMC wing panel section. The silicon carbide fibers in TMC are formed by vaporization of silicon carbide on a graphite filamant. The fibers are then coated with a carbon-rich layer. The skin sheet in Fig. 4 is a laminate

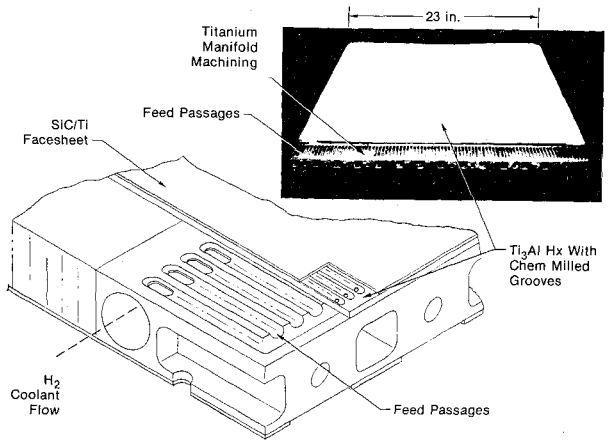

Fig. 5 Actively cooled nozzle panel section.[2]

of seven lamina (layers) of alternating 0 deg/90 deg fibers. The TMC hat-stiffener sheet is diffusion bonded to the skin.

The nozzle is defined as that portion of the vehicle starting aft of the engine and continuing on to the aft fuselage closeout. The nozzle skin structural concept is an actively cooled panel as shown in Fig. 5. Active cooling is achieved using liquid hydrogen which is passed through channels milled into the face sheets before entering the engine. The actively cooled panel core is titanium. The face sheets are advanced titanium matrix composites. The panels are 48-in. (1.2-m) square. The panels are supported by advanced titanium matrix composite frames, which are in turn attached to the underlying structures. The actively cooled honeycomb sandwich was selected in consideration of the extreme temperatures and heat fluxes from the engine exhaust—conditions which make passively cooled structures untenable in the nozzle region. However, ongoing evaluations indicate a possible chemical incompatibility between titanium and liquid hydrogen. Thus, use of materials other than titanium may be required for actively cooled panels.

Aerothermal Analysis of Skin Panels

Aerothermal and aeroacoustic loads are produced by the external flow of air. As the vehicle flies at hypersonic speeds, air is adiabatically compressed by its own momentum along the vehicle contours. Aerothermal heating and aeroacoustic pressure fluctuations are produced in the boundary layer. As shown in Fig. 6, the bow shock forms forward of the vehicle and, at hypersonic speeds, bends aft in a parabolic cone which impinges on vehicle wing and tail. As shown in Fig. 7, shock waves impingement on the boundary layer amplifies the boundary-layer pressure fluctuations and can produce heating and fluctuating pressures an order of magnitude higher than those without shock impingement.[5,6] A similar amplification of boundary-layer pressure fluctuations is produced by separated flow. However, data for these effects are very limited. Algorithms available for predicting aeroacoustic and aerothermal loads are limited by the absence of data above Mach 8.[4,5]

The attached flowfield over a two-dimensional representation of the vehicle was predicted using a parabolized Navier-Stokes (PNS) code as shown in Fig. 8. The code uses a K-ε turbulence closure model and incorporates real gas effects. The PNS code gives a direct prediction of the attached boundary-layer thickness, the heating within the boundary layer, and the external flowfield at each point in the trajectory. The PNS solution was also used to provide the approach flow conditions for shock-boundary-layer interaction. Nozzle loads were determined by a separate analysis of the burning gases. Typical peak heat flux on the nozzle was computed to be 250 BTU/ft^2-s (2.83 MW/m^2) at the combustor exit, with an average value of 180 BTU/ft^2-s (2.0 MW/m^2). This nozzle heat

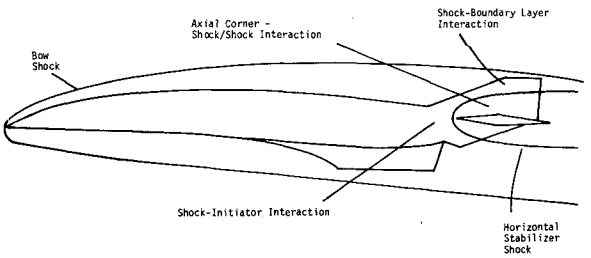

Fig. 6 Shock waves impinging upon vehicle skin panels.[5]

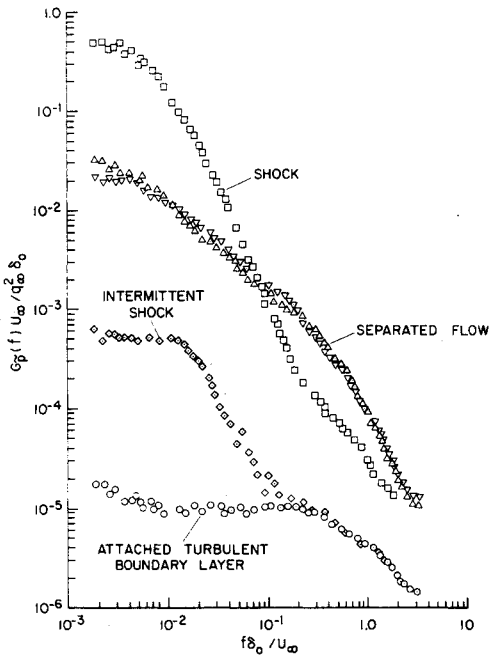

Fig. 7 Typical power spectra of pressure fluctuations underlying supersonic flow.[6] $G_p(f)$ = power spectral density of pressure fluctuations; δ = boundary-layer thickness; U_∞ = freestream velocity.

flux is 10 times greater than the heat flux associated with attached turbulent boundary layer on the remainder of the vehicle (Fig. 9). The nozzle heat flux would lead to temperatures in excess of 3000°F (1650°C) on nozzle skin panels if active cooling were not provided.

There is significant uncertainty in predicting the transition between laminar and turbulent boundary layers in hypersonic flow. For example, surveys have shown that three-dimensional geometries have different transition behavior than two-dimensional shapes.[7] Moreover, the Reynolds numbers decrease during ascent, so there is a tendency for the turbulent boundary layer on the forebody to relaminarize as the vehicle ascends. Since heat and aeroacoustic loads are an order of magnitude greater for turbulent boundary layers than for laminar boundary layers, location of boundary-layer transition has a major impact on loads, material choice, and design of skin panels.

Laganelli et al.[4] have shown that the spectrum and overall root-mean-square (rms) of the fluctuating pressure in an attached, hypersonic, turbulent boundary layer are a function of the Mach number at the edge of the boundary layer, boundary-layer geometry, and heat transfer at the wall.[4] The fluctuating pressures on the vehicle skin due to the attached turbulent boundary layer are shown in Fig. 9. The overall sound pressure levels in the attached boundary layer without shock impingement range from 120 to 150 dB. The highest levels are in the nosetip region and along the ramp toward the inlet. The spectrum of the boundary-layer pressure fluctuations is broadband and flat to approximately 10,000 Hz, rolling off at higher frequencies.

A detailed investigation was made of the impingement of the bow shock on the wing (Fig. 6). The wing extends 12 deg from the vehicle axis. As speed increases, the bow shock bends aft toward the wing. For speeds in excess of Mach 10, the bow shock impinges on the wing. Available experimental data show that shock-boundary-layer interaction is a function of shock strength. Increases in heat flux, as well as fluctuating pressure of 10–45 dB, have been observed when a shock impinges on a turbulent boundary layer.[6,8,9] Laganelli and Wolfe[5] have developed correlations for shock impingement heat flux and fluctuating pressure as a function of the shock

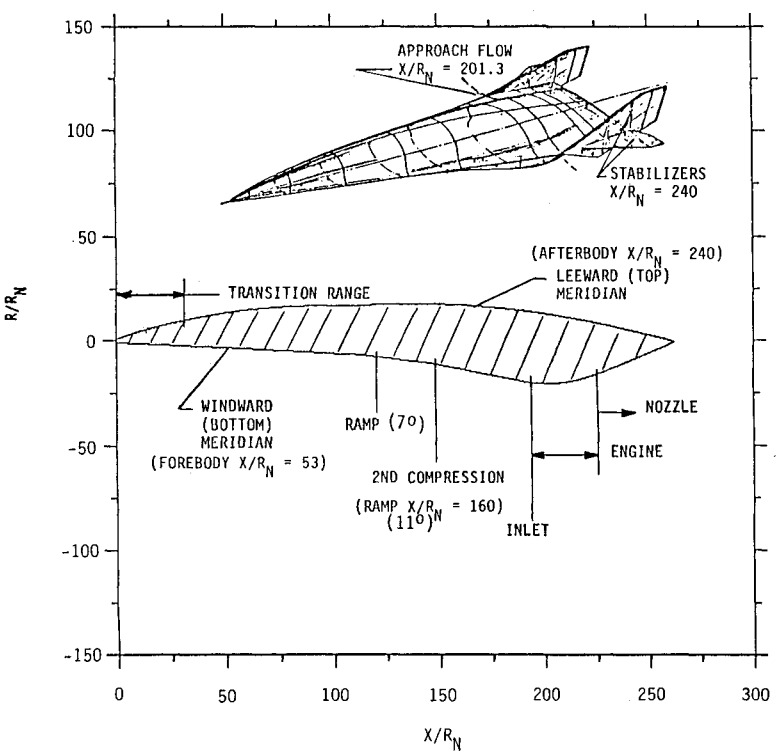

CONDITIONS *

R_N = 4.5 INCHES

Q_∞ = 1000 PSF

M_∞	ALT (KFT)	X_{TR} (FT)	T_w (°R)	SURFACE
4	71	6	540	B/T
6	88.4	6	1600	B/T
			2000	B/T
10	110.9	12	1600	B/T
15	129.9	15	1600	B/T
20	144.1	0	1600	B/T
25	155.7	0	1600	B/T

Q_∞ = 2600 PSF

6	68.0	0	1600	B
10	89.75	0	1600	B/T
15	107.6	0	1600	B
20	120.5	0	1600	B
25	131.5	0	1600	B

B - Bottom (Windward)
T - Top (Leeward)

Fig. 8 Two-dimensional model for PNS flowfield solution.

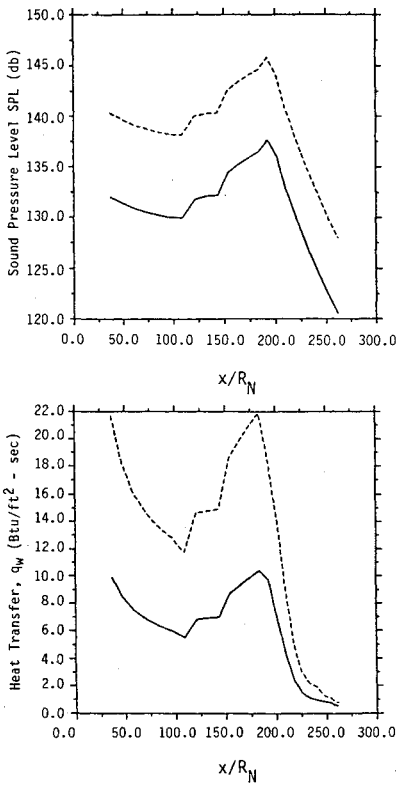

Fig. 9 Thermal and acoustic loads on windward surface of BWB at Mach 10. --- = 2600q ascent, —— = 1000q ascent; x/R_N = vehicle station (Fig. 8).

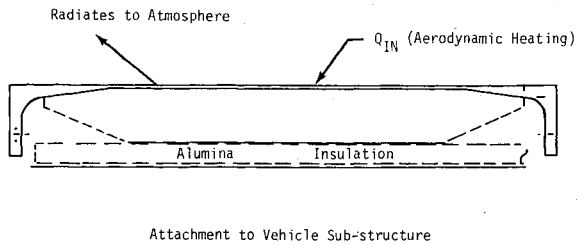

Fig. 10 Thermal analysis of forebody panel.

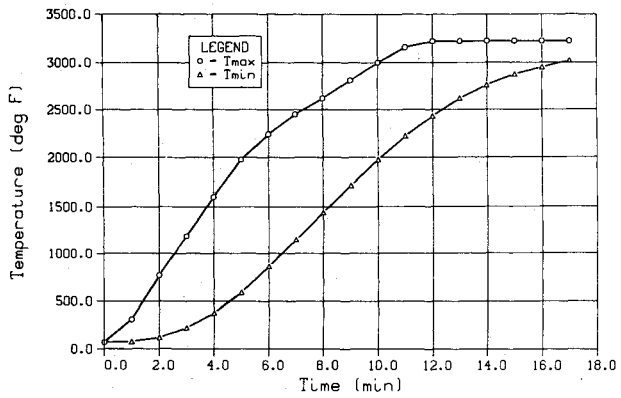

Fig. 11 Forebody panel temperature rise for 1000q ascent.

strength.[5] Their correlation predicts that the rms fluctuating skin pressure at shock impingement is 166 dB, with a peak local heat flux of 92.5 BTU/ft²-s (1.05 MW/m²) at Mach 20 in the 1000q ascent trajectory. These loads increase by a factor of two for the 2600q ascent. In the absence of shock impingement, the heat flux for the 1000q ascent is 20 BTU/ft²-s (0.22 MW/m²) and the fluctuating pressure is only 140 dB (Fig. 9). Thus, location of shock impingement is critical to the design of hypersonic vehicle skin panels.

Transient thermal analysis of the carbon-carbon skin panels was made to determine skin panel temperatures during ascent to orbit. The panels receive thermal energy from aerodynamic heating of their surface and reradiate this thermal energy into space (Fig. 10). An alumina insulation blanket is placed between the panel and the substructure to limit convective heat transfer into the substructure. Temperature gradients through the thin, highly conductive carbon-carbon skin are negligible, but temperature differences between the skin and the cooled substructure attachment are high, in the 1200–1400°F (650–760°C) range. Fortunately, the in-plane thermal expansion coefficient of carbon-carbon is very low, on the order of 1×10^{-6} in./in.-°F (0.6×10^{-6} mm/mm-°C), so these large temperature differences do not induce unacceptable thermal stresses.

A detailed transient analysis of the forebody and ramp panels was made using finite element methods with the transient mission heat loads developed in the previous section. Temperature rise of the forebody panel due to aerodynamic heating of the attached boundary layer during ascent is given in Fig. 11. The maximum temperature rise occurs at the center of the skin bay. The minimum temperature rise occurs adjacent to the substructure attachments. For the 1000q ascent, the calculated peak temperature is 2670°F (1460°C) for the forebody and 2510°F (1375°C) for the ramp. For the 2600q case, the corresponding peak temperatures of 3250°F (1790°C) and 3010°F (1650°C), are above the 3000°F (1650°C) maximum-use temperature for carbon-carbon. If the flow relaminarizes, maximum temperatures are reduced by 1200°F (650°C) to a maximum of 2050°F (1140°C), which is within the temperature range of carbon-carbon. Thus, analysis of laminar/turbulent transition and heat flux is critical in the design of the forebody and ramp panels.

Engine Acoustic Loads

The BWB hypersonic vehicle has rocket engine thruster modules mounted in twin rows across the tail as shown in Fig. 2. The thrusters are used to reach speeds Mach 2 to 3, at which point the scramjet becomes efficient. The noisiest portion of the flight occurs during takeoff when the rocket engines and the scramjet engine are both operating. Sound levels on the lower half of the vehicle are higher than on the upper half of the vehicle owing to reflections from the runway, as well as direct acoustic radiation from the lower midbody mounted scramjet.

Both NASA[10] and Von Gierke[11] have developed models for rocket engine noise based on the exhaust power of the engine. The NASA technique assumes that the overall acoustic power is equal to 1% of the overall fluid power. Assuming that the thrusters exert a total thrust of 400,000 lb (1.8 MN) with an exhaust gas velocity of 20,000 ft/s (6000 m/s), the NASA technique gives an overall acoustic power of 194 dB relative to 10^{-12} W. The Von Gierke technique gives a slightly higher result. The sound power produced by the scram jet engine is approximately the same as that produced by the thrusters, but its maximum sound power occurs at lower frequencies owing to its larger dimensions. The engines sound spectrum is relatively flat between 500–5000 Hz as the high-frequency noise from the rocket thrusters combines with the lower frequency noise from the scramjet.

A directivity index was used to determine off-axis sound levels.[12] Reflection from the ground was taken into account to estimate overall sound levels on the vehicle skin during takeoff as shown in Fig. 12. Direct radiation from the engines results in overall sound pressure levels in the 170–180 dB range (relative to 20 μPa) on skin panels in the inlet and exhaust regions. These levels are comparable to the highest level measured in turbojet engines. As shown in Table 1, engine loads are considerably higher than the attached turbulent boundary-layer loads, and they are comparable to shock impingement loads.

Table 1 Typical maximum aeroacoustic loads at Mach 10 for q = 2600 ascent

Loading	Overall SPL, dB[a]	Heat flux, BTU/ft^2-s
Attached turbulent boundary layer	145	22
Shock impingement on boundary layer	167	49
Engine exhaust on nozzle at takeoff thrust	176	100

[a]Re 20 μPa

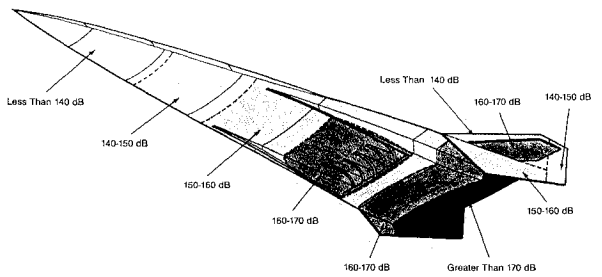

Fig. 12 Overall sound pressure levels relative to 20 μPa due to engine noise at takeoff.

Skin Panel Static and Dynamic Analysis

Static and dynamic analyses of the forebody, ramp, and actively cooled panels were made using the MSC/NASTRAN finite element code. For the forebody and ramp panels, the quadralateral plate element was used with carbon-carbon material properties determined from test. Mean (i.e., static) loads on the panels are of three types: 1) thermal loads associated with aerodynamic heating of the panel surface; 2) aerodynamic pressure loads applied directly to the skin; and 3) vehicle carry-through loads imposed at the panel boundaries by vehicle deformation and maneuvers. Thermally induced loads are generally highest when vehicle temperature is greatest, which occurs when the vehicle is at the top of the ascent trajectory (Fig. 11).

The highest stresses in the forebody panel are generated by vehicle carry-through in-plane loads imposed by the fasteners between panels. The forebody panel design, shown in Fig. 3, is marginal for buckling under in-plane loads. Rotating the panel by 90 deg, so that the stiffeners are 90 deg to the imposed loads, would lead to panel buckling. On the other hand, the ramp panel, which is designed as a heat shield and bears no vehicle carry-through loads, has its highest stress at the top of the stiffeners, and it is not critical for static loads.

Dynamic analysis of the forebody and ramp panels was made by first calculating the mode shapes and natural frequencies of the panels, and then determining the dynamic response to fluctuating surface pressures in each mode. For the forebody panel, the effect of the carry-through loads imposed by the fasteners was incorporated using a nonlinear solution. Modal analysis shows that the panel modes are generally of two types as shown in Fig. 13: 1) modes where adjacent panel bays deflect inphase, and 2) modes where adjacent bays deflect out of phase, causing the intermediate stiffener to rotate. The lowest frequency mode of the forebody panel was at 524 Hz, with in-phase motion of adjacent bays. The ramp panel, which has wider stiffener spacing and thinner skin gauge than the forebody panel, has an out-of-phase mode at 258 Hz.

The forebody and ramp panels respond to engine noise and aeroacoustic loads. Aeroacoustic analysis shows that the maximum aeroacoustic fluctuating pressures due to boundary-layer turbulence on the forebody panel fall in the 130–145 dB range, a factor of 3–6 smaller than the engine sound pressure levels of 155–160 dB. The engine noise at the ramp

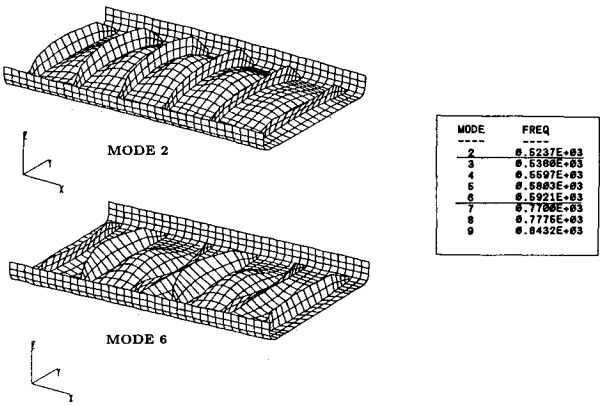

Fig. 13 Forebody panel in-phase and out-of-phase vibration modes.

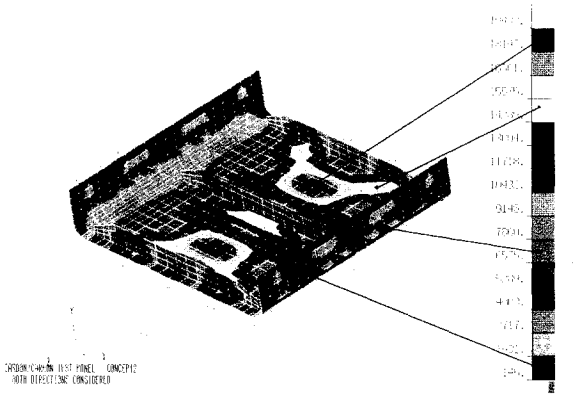

Fig. 14 Ramp panel carbon-carbon sonic fatigue rms stress field.

panel is estimated at 160–170 dB. Shock waves emanating from the inlet can impinge on the ramp to generate fluctuating pressures that equal or exceed the engine noise on the ramp panel. Both the engine noise and the shock impingement loads exceed attached turbulent boundary-layer loads on the ramp panel.

The analytical approach used to determine the response of the panels to the random pressures imposed by the turbulent boundary layer and engine noise is based on an extension of earlier work to include higher modes.[13,14] The panel response is proportional to rms fluctuating pressure multiplied by the joint acceptance of the acoustic field of the panel modes. The joint acceptance of engine noise by each panel mode was estimated by considering the wavelength of the sound waves, weighted by the wavelength of panel modes. The stresses in each mode were summed to produce an overall stress level. The resultant distribution of stresses for the ramp panel is shown in Fig. 14. The maximum acoustic stresses occur in the skin at the center of the panel bays. For the forebody panel, the maximum cyclic stress is 4000 psi (27.6 MPa) rms and is within the 6000 psi (41.4 MPa) rms random vibration fatigue allowable for carbon-carbon. The calculated maximum ramp panel stress of 16,080 psi (111 MPa) rms is over two-and-half times the carbon-carbon allowable. As a result, either the skin gauge of the proposed ramp panel must be increased, or stiffener spacing must be decreased to avoid in-service failure due to engine noise.

NASTRAN finite element dynamic analysis of the actively cooled panel shows that the fundamental bending mode occurs at 82 Hz. This relatively low frequency, and the associated low stiffness, results from the 48-in. (1.2-m) span of the panel. The maximum stresses occur on the inner face sheet at the center of the panel. While the panel can bear the mean aerodynamic and carry-through loads imposed on it, the engine-induced acoustic loads at takeoff exceed the fatigue ca-

pability of the panel. Additional analysis suggests that by incorporating intermediate supports at 12-in. (30.5-cm) intervals, the stresses will be reduced below the fatigue allowable. Because the actively cooled panel contains pressurized combustible hydrogen, it may require higher margins of safety than other panels.

Discussion

Skin panels are sized both by aerothermal loads imposed directly on the panel surface by the airstream, and by loads imposed at the panel boundaries by the remainder of the vehicle. Experience shows that if a panel is designed for primary load and stiffness, it will not be design-critical for aeroacoustic loads. However, if a skin panel serves primarily as an aerodynamic fairing rather than as a load bearing structure (e.g., ramp panels), then aerothermal and acoustic loads applied directly to its surface will size the panel. The transatmospheric hypersonic vehicle is unusual in that so many of its skin panels are directly exposed to high aerothermal, aeroacoustic, and engine acoustic loads. The high heat fluxes caused by shock impingement will require local ceramic heat shields or active cooling. Such features would not be required on a conventional aircraft.

A typical design life objective for a hypersonic research vehicle is 100 flights. The design-critical loading is dominated by the 15-min ascent portion of the flight. Approximately 12 min of the ascent is spent under scram jet power and 3 min under rocket power. Thus, to meet a 100 flight life, a skin panel must endure 100 thermal cycles, 1200 min at high temperature exposed to shock interactions, and 300 min exposed to rocket engine loads. The panels will accumulate over 20 million vibration cycles during the 100 flights.

Failure of the panel can occur from acoustic and vibration loads (high-cycle fatigue), from flight cycle thermal and mechanical loads (low-cycle fatigue), or from material deterioration due to excessive temperature (oxidation). The maximum aerothermal heat fluxes and shock impingement fluctuating pressures occur simultaneously. High thermal mean stress reduces the allowable for high-cycle fatigue. High temperature reduces the fatigue allowable of metals. It is often difficult or impossible to determine whether a failure under heat and vibration had its origins in high-thermal mean stress, in vibration, or in excessive temperature. Vibration-induced deterioration of a coating can also lead to an oxidation failure. As a result of these damaging interactions between thermal and acoustic loads, it becomes necessary to analyze and test panels under simultaneous heat and vibration.

Facilities which can simultaneously apply aerothermal heat flux and aeroacoustic pressure fluctuations on panels are needed to validate designs and materials. A heated progressive acoustic wave tube has been constructed at Rohr Industries which uses quartz lamps to achieve 2000°F (1090°C) over a 33 by 23 in. (0.83 by 0.58 m) test section with 170 dB overall sound pressure level. The facility was designed for testing the panels shown in Figs. 3–5.

Conclusions

An analytical study was made of vibroacoustic fatigue of hypersonic flight vehicle skin panels. A single-stage-to-orbit mission and BWB vehicle were developed which are representative of present transatmospheric vehicle design studies. The external flowfield and boundary-layer heating were determined by parabolized Navier-Stokes flow analysis. Engine acoustic loads were developed. Detailed thermal, static, and dynamic analyses have been made of the forebody, ramp, and nozzle panels.

The study shows that engine acoustic loads and shock-impingement loads will govern the design of many skin panels. The conclusions of the study are as follows:

1) Overall aeroacoustic sound pressure levels on the skin for attached turbulent boundary layers range between 120–150 dB, relative to 20 μPa. These attached turbulent boundary-layer loads will be exceeded both by engine acoustic and shock impingement loads. Maximum engine-induced acoustic loads occur at takeoff and act on components in line-of-sight of the engine inlet and exhaust. The maximum engine acoustic sound presure levels range between 170–180 dB overall. At hypersonic speeds, shock waves bend aft from the bow and from the inlet, and impinge on wing, tail, and ramp skin panels. The maximum shock-boundary-layer interaction fluctuating surface pressures are between 160–170 dB and will be accompanied by local heat fluxes as high as 50 BTU/ft^2-s (0.6 MW/m^2).

2) Finite element analysis of the 0.15-in. (3.8-mm) thick carbon-carbon forebody skin panel shows that the maximum skin temperature is 2667°F (1460°C) at the end of a 1000q ascent, and 3220°F (1770°C) for a 2600q ascent. These results are based on turbulent boundary-layer heating. If a laminar boundary layer exists, the temperatures can be 1200°F (650°C) lower. The high vehicle carry-through loads dominate the design of the forebody panel. Sufficient stiffness is required to prevent buckling. Stresses induced by the attached turbulent boundary layer and the inlet noise are below the fatigue allowable for carbon-carbon.

3) The 0.065-in. (1.65-mm) thick carbon-carbon ramp panel is a heat shield which carries no vehicle carry-through loads. Maximum temperature at the end of ascent is 2510°F (1380°C) for the 1000q ascent, and 3020°F (1660°C) for the 2600q ascent. Maximum stress due to 165-dB engine noise radiated from the scramjet inlet is 16,100 psi (111 MPa) rms, which is well above the high cycle fatigue allowable for carbon-carbon. Thus, gauge increases or additional stiffeners are required to design this panel to withstand aeroacoustic and engine noise loads.

4) While finite element analysis has not been conducted on either the titanium metal matrix aftbody or on the wing and vertical stabilizer panels, preliminary analysis indicates that shock impingement will be the design-governing loads for many of these panels.

5) Finite element analysis of the actively cooled nozzle panel shows that the highest acoustic stress is at the center of the inner face sheet. The manifolds are not stiff enough to provide good edge fixity. As a result, the panel responds as if it were simply-supported. With 48-in. (1.2-m) proposed support spacing, the acoustic takeoff loads will cause high-cycle fatigue failure of the actively cooled panel considered in this study.

Acknowledgments

This article reports work sponsored by the Flight Dynamics Laboratory, Wright-Patterson Air Force Base, and performed by a team from Rohr Industries, San Diego, California, McDonnell Douglas, St. Louis, Missouri, and Science Applications International, Ft. Washington, Pennsylvania. Peter Pozefsky led the McDonnell Douglas effort and contributed airframe, performance, and actively cooled panel analysis. Anthony L. Laganelli of SAIC led the computational fluid dynamics and aerothermal analyses. Sarunas Landys edited the manuscript.

References

[1]"Report of the Defense Science Board Task Force on the National Aerospace Plane (NASP)," Dept. of Defense, AD-A201-124, Washington, DC, Sept. 1988.

[2]Pozefsky, P., Blevins, R. D., and Laganelli, A. L., "Thermo-Vibro-Acoustic Loads and Fatigue of Hypersonic Flight Vehicle Structure," Air Force Wright Aeronautical Lab., TR-89-3014, Flight Dynamics Lab., Wright-Patterson AFB, OH, Feb. 1989.

[3]Tauber, M. E., Menees, G. P., and Adelman, H. G., "Aerodynamics of Transatmospheric Vehicles," *Journal of Aircraft*, Vol. 24, No. 9, 1987, pp. 594–602.

[4]Laganelli, A. L., Martellucci, A., and Shaw, L. L., "Wall Pressure Fluctuations in Attached Boundary Layer Flow," *AIAA Journal*, Vol.

21, 1983, pp. 495–502; see also Air Force Flight Dynamics Lab. TR-77-59.

[5]Laganelli, A. L., Wolfe, H. W., and Wentz, K. R., "Prediction of Fluctuating Pressure in Attached and Separated Compressible Flow," 31st Aerospace Sciences Meeting, AIAA Paper 93-0286, Reno, NV, Jan. 1989.

[6]Coe, C. F., Chyu, W. J., and Dods, J. B., "Pressure Fluctuations Underlying Attached and Separated Supersonic Turbulent Boundary Layers and Shock Waves," AIAA Aeroacoustics Conf., AIAA Paper 73-996, Seattle, WA, Oct. 1973.

[7]Berkowitz, A. M., and Kyriss, C. L., "Boundary Layer Transition Study, Volume I, Task 1 Final Report—Correlation of Flight Test Transition Onset and Movement Data," Air Force Flight Dynamics Lab. TR-78-4, Wright Patterson AFB, OH, July 1978.

[8]Zorumski, W. E., "Fluctuating Pressure Loads Under High Speed Boundary Layers," NASA TM 100517, Oct. 1987.

[9]Tran, T. T., Tran, D. K., and Bogdonoff, S. M., "Surface Pressure Fluctuations in Three-Dimensional Shock Wave Turbulent Boundary Layer Interactions at Various Shock Strengths," AIAA Paper 85-1562, July 1985.

[10]Eldred, K. M., "Acoustic Loads Generated by the Propulsion System," NASA SP-8072, June 1971.

[11]Von Gierke, H. E., "Aircraft Noise Sources," *Handbook of Noise Control*, edited by C. M. Harris, McGraw-Hill, New York, 1957, Chap. 33.

[12]McInerny, S., "Rocket Noise—A Review," AIAA 13th Aeroacoustics Conf., Tallahasse, FL, Oct. 1990.

[13]Blevins, R. D., "An Approximate Method for Sonic Fatigue Analysis of Plate and Shell Structures," *Journal of Sound and Vibration*, Vol. 129, No. 1, 1989, pp. 51–71.

[14]Blevins, R. D., "Flow-Induced Vibration," 2nd ed., Van Nostrand Reinhold, New York, 1990.